Computational Model of Ductal Carcinoma In-Situ

Seth Shumate[1] and Magda El-Shenawee[2]

[1] Microelectronics-Photonics Program
University of Arkansas, Fayetteville, AR 72701, USA
sshumat@uark.edu

[2] Department of Electrical Engineering
University of Arkansas, Fayetteville, AR 72701, USA
magda@uark.edu

Abstract: Breast cancer, when found in its early stages, is a manageable disease. When detected, biopsied, and diagnosed, lesions such as ductal carcinoma *in-situ* (DCIS) or invasive ductal carcinoma (IDC) are promptly removed. Consequently, the natural history of DCIS and IDC *in-vivo* is not well known. DCIS manifests itself with various distinctive patterns and pathologies. In order to study the growth differences between these types of the *in-situ* disease, namely papillary, cribriform, solid, and comedo, a cellular automaton model has been developed. The model's focus has been placed on observed cellular phenomenon which have been identified via traditional *in-vitro*, animal, and histological studies of DCIS. Two scenarios for the model are compared here: one in which the luminal epithelial cells contribute to contact inhibition of the cancerous cells and one where they do not. Differing growth characteristics will be discussed for each simulated scenario.

Keywords: Ductal carcinoma *in-situ,* DCIS, tumorigenesis, and contact inhibition.

1. Introduction

All human cancers have mutations which promote tumor growth, invasion, and metastasis [1]. Ductal carcinoma *in-situ* (DCIS) is a precancerous growth of luminal mammary epithelial cells. Cells that compose ductal carcinoma, similar to other types of cancer, lose the ability to normally regulate proliferation. In addition, cells acquire other mutations, such as recruiting a new blood supply and local tissue invasion. Invasive ductal carcinoma (IDC) accounts for 75% of all cases of breast cancer. Incidence rates of DCIS detection have been increasing in large part because of mammographic screening. When DCIS is detected, the standard treatment includes diagnostic biopsy, removal, and subsequent treatment. Consequently, studying the disease has traditionally been limited to *in-vitro* and animal models. The purpose of the model presented here is to investigate the growth and pattern formation of the different types of DCIS: papillary, cribriform, solid, and comedo.

Theoretical biology, a blend of biology, mathematics, and computer science, has also emerged as a method for studying tumor growth. Several models exist which examine various aspects of DCIS [2]-[6]. Only the model developed by Xu [6] attempted to reproduce DCIS patterns, with the exception of comedo-type DCIS. In the model, the tumor growth was described mathematically as the flow of nutrients within a cylinder on a two-dimensional scale [6]. The model proposes that it is only nutrients responsible for the complex shapes associated with DCIS [6]. While nutrient concentration does play a role in the formation of the necrotic core in comedo DCIS, Xu's model does not incorporate the process

of cell death or comedo DCIS [6]. Contrarily, the focus of the model proposed here is placed on observed biological processes that affect normal and abnormal epithelial cell growth and organization.

Myoepithelial and luminal epithelial cells of the mammary ducts are arranged in single cell layers, with the myoepithelial cell layer surrounding the epithelial cell layer. Beyond the myoepithelial layer is the basement membrane which gives mechanical support to the duct and also acts as a barrier to DCIS invading the surrounding tissue. Healthy luminal epithelial cells are connected to one another by E-Cadherin, a cell adhesion molecule. Proper E-Cadherin contact is largely responsible for the maintenance of the luminal epithelial layer. When a normal epithelial cell is surrounded laterally by other epithelial cells, then the cell will not grow, thus forming a sheet of cells. This mechanism is called contact inhibition. E-Cadherin has been identified as an essential component of contact inhibition [7]. Normal E-Cadherin expression has also been found to be reduced in both low grade and comedo DCIS [8]. Papillary, cribriform, and solid DCIS are considered low grade forms of the disease marked by well differentiated cells. The characteristic papillary pattern presents finger-like growths projected inward towards the center of the lumen. Cribriform has a punctate, 'swiss cheese' pattern. Both solid and comedo fill the lumen, but comedo DCIS, being more aggressive, distends the duct wall and has a central area of necrotic cells called the necrotic core.

Although the exact genetic or mutational events leading to these remarkably different patterns have yet to be verified, the model presented here focuses on the decrease in E-Cadherin expression as a major contributing factor. Whether or not the loss of E-Cadherin in DCIS cells occurs as a result of genetic mutation or some influence from the local tissue environment is not clear. Regardless, the idea presented here is that the pro-growth signals begin to outweigh the normal E-Cadherin mediated contact-inhibition mechanism, leading to abnormal proliferation. The model described in the following sections produces patterns that closely resemble clinically observed lesions.

2. Methodology

A. Discretization

The model is a cellular automaton where cell sites are placed in a hexagonal lattice configuration. Each site has six neighboring sites, and the future state of any site is dependent upon the current state of that and the surrounding sites. All site types share nutrients with immediate neighbors. A single-cell boundary of healthy epithelium makes up the duct. Myoepithelial cells and the basement membrane were not modeled, but would be essential for modeling the progression from *in-situ* to invasive ductal carcinoma. Outside of the duct, a site represents either a capillary or stromal tissue. Capillary sites act as the source of a generic nutrient and are not located inside the duct. According to Nacarrato, et al., approximately 29% of the area surrounding the duct is occupied by blood vessels [9]. Therefore, capillary sites are randomly initialized at 29% of the extraductal sites. The duct is centered at (150, 150) on a 300 x 300 grid. An initial cancer seed is placed on the edge of the duct. All other sites within the duct start as luminal fluid which can be replaced by cancer cells, given cell division is allowed.

B. Nutrient Diffusion

All site types are given initial nutrient concentrations. These values and the values for other parameters are given in Table 1. This system is modified from a model by Sansone, et al [10]. Only capillaries are able to renew their nutrient supply each iteration to the initial concentration, while levels at other sites can reach very low values depending on the concentration of cancer cells present. The upcoming nutrient concentration at any site is determined each iteration by:

$$p_{ij}^{t+1} = p_{ij}^{t} + \sum_{i'j'}^{NN} (\alpha_{ij} p_{i'j'}^{t} - \alpha_{i'j'} p_{ij}^{t}) - \gamma_{ij}^{t} - \xi_{ij} + \psi_{ij}^{t} \quad (1)$$

Table 1: Parameters and initial values

Parameter	**Value**	**Description**
α_{ij}	0.166	Nutrient diffusion coefficient for all tissue types.
ξ_{ij}^{t}	0.002 0.001	Stromal tissue nutrient intake Capillary nutrient intake
Γ	0.006	Max. nutrient intake by cancer cells
β	0.005	Metabolic rate for cancer cells
Q_m	0.015	Mitotic nutrient threshold
$p_{ij}^{t=0}$	50.0 8.85	Initial nutrient concentration: Capillaries Other sites

where p_{ij}^{t} is the current concentration, $\sum_{i'j'}^{NN}$ is the summation over the neighboring sites (i', j'), α_{ij} is the tissue diffusion coefficient, assumed in this model to be the same for all sites, γ_{ij}^{t} is the nutrients consumed by a cancer cell, ξ_{ij} is the amount of nutrient consumed by a healthy cell, and ψ_{ij}^{t} is the amount of nutrient needed to restore the initial level at capillary sites.

C. Cell Cycle

The healthy epithelial cells, stromal cells, and capillaries consume a constant amount of nutrients, ξ_{ij}. These sites, unlike cancer cells in the model, do not die or divide. Cancer cell sites uptake a variable level of nutrients:

$$\gamma_{ij}^{t} = \Gamma\left[1 - e^{\left(-\frac{p_{ij}^{t}}{\Gamma}\right)}\right] \tag{2}$$

where Γ is the maximum amount of nutrients that the cancer cell can consume in one iteration. This system is also modified from [10]. Once available to the cell, a constant amount of nutrients, β, is used for metabolic processes. Any excess is stored within the cell, where σ_{ij}^{t} represents the nutrient storage. Depending on the recently consumed and stored nutrient levels compared to β, the cancer cell will either divide, remain quiescent, enter a hypoxic state, or die:

$$If\ \sigma_{ij}^{t} + \gamma_{ij}^{t} - \beta \begin{cases} \geq Q_m & Divide \\ > 0\ and\ < Q_m & Quiescent \\ \leq 0 & Hypoxia\ /\ Necrosis \end{cases} \tag{3}$$

where Q_m is the mitotic threshold. When the cell enters a hypoxic state, its nutrient requirements drop from β to $\beta/4$. The percent chance of necrosis increases every iteration that the nutrients available to the cell is less than $\beta/4$ proportional to $\left(\sigma_{ij}^t + \gamma_{ij}^t\right)/\beta$. If the cell dies, the site will become luminal after 200 iterations when four or more of its neighbors are non-necrotic cells. Otherwise, the necrotic cell will coagulate with neighboring necrotic cells.

Cells that have enough nutrients to divide can only do so dependent upon their level of E-Cadherin expression. This is modeled by assigning a number to each cancer cell in a range from two to six. During any one simulation, this number will only be between two consecutive integers as a probability of being one or the other. Also, a single value from two to six can be assigned during a simulation with 100% probability. This number will be called the Neighboring Cell Number (NCN), and probabilities will be denoted by, for example, NCN_2 = 100 %. A simulation beginning with NCN_2 = 100% means that the cancer cells will only be able to divide if the number of cells they contact is less than two. If a two-dimensional cross-section of a healthy duct were examined, each cell would have two neighbors. Healthy epithelial cells fully express E-Cadherin. Therefore, if a cancer cell has NCN_2 = 100%, then it is most like a normal epithelial cell. The cases examined in this work have combinations of NCN_3 and NCN_4. This combination produces cribriform patterns. Two scenarios are examined and compared here varying the combination of these values.

D. Contact Inhibition and the Luminal Epithelial Layer

Both scenarios employ the same parameters as given in Table 1. The first scenario considers the luminal epithelial cells able to contribute to contact inhibition. When a cancer cell is contacting one of the healthy epithelial cells, this cell is included in determining whether or not the cancer cell can divide. The second case does not include the ductal boundary cells in the neighbors that can inhibit cancer cell growth. In Fig. 1 the bold cancer cell (C) is in direct contact with one other cancer cell (C) as well as two normal epithelial cells (E). In scenario one, the bold cancer cell would not be able to divide since the number of neighboring cells is equal to the cancer cell's NCN = 3 value. In scenario two, however, this same cell would be able to divide into a surrounding luminal (L) site since the cancer cell is only inhibited by contact with other cancer cells.

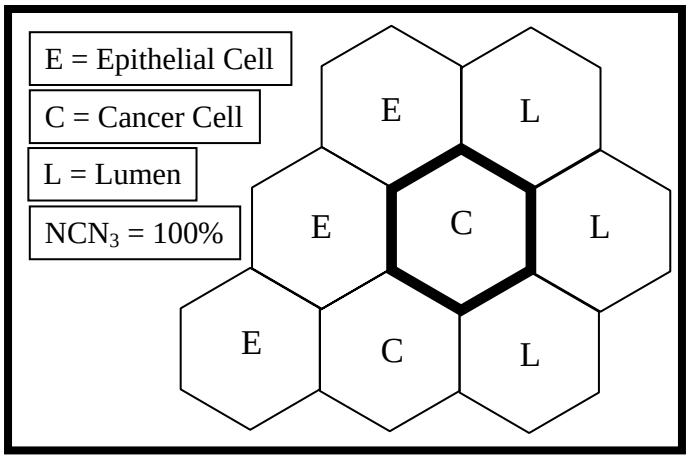

Fig. 1. Example of contact inhibition for two scenarios with NCN = 3 at 100% probability.

3. Results and Discussion

Both scenarios are simulated for NCN_4 = 100%, 2%, 1%, 0.67%, 0.5%, 0.4%, 0.33%, and 0.28% with corresponding NCN_3 = 0%, 98%, 99%, etc. Table 2 lists the NCN_4 values as well as final population and the iterations required to end the simulation. Simulations end when no possible spaces can be filled.

Table 2: Data for both scenarios with varying NCN values.

Scenario 1			Scenario 2		
NCN = 4	Iterations	Population (cells)	NCN=4	Iterations	Population (cells)
100%	900	1047	100%	1000	1166
2%	4000	1044	2%	4000	1064
1%	6300	1021	1%	5100	1119
0.67%	9600	1001	0.67%	4400	1105
0.50%	15000	953	0.50%	6500	1061
0.40%	13900	1012	0.40%	9000	1063
0.33%	16900	978	0.33%	11400	1096
0.29%	25500	1037	0.29%	16000	1067

Although within each scenario there is no significant trend in terms of final cancer cell population, lowering the probability of NCN_4 generally causes a greater increase in time to completion. As seen in Figs. 2 and 3, when the luminal epithelial cells contributed to contact inhibition (scenario one), reaching a stable configuration takes many more iterations compared to scenario two. This is because proliferation in the second scenario is easier along the duct, which causes a clinging, papillary, and then cribriform pattern.

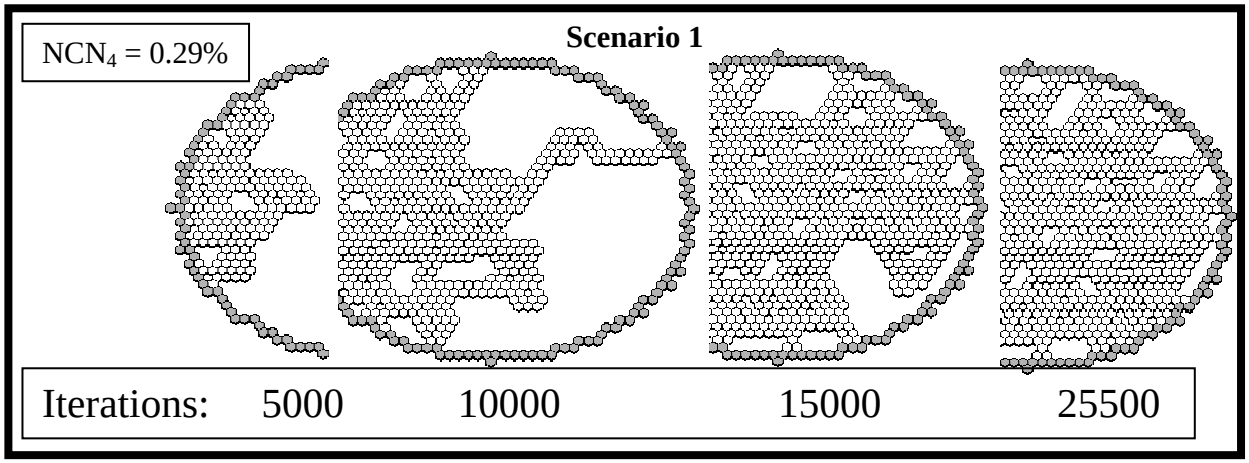

Fig. 2. Cribriform type growth where luminal epithelial cells contribute to contact-inhibition.

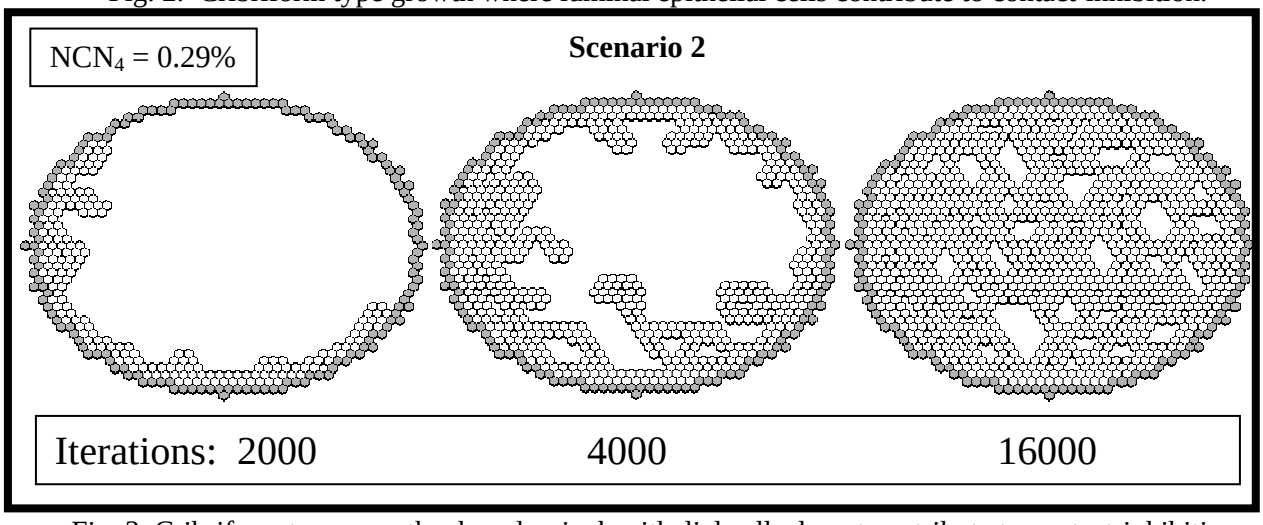

Fig. 3 Cribriform type growth where luminal epithelial cells do not contribute to contact-inhibition.

4. Conclusions

The differences in morphology and growth characteristics between both scenarios considered here provide interesting insights into the possibilities of DCIS. The different patterns of DCIS are thought to be separate entities. Perhaps the only difference between papillary and cribriform patterns is the mitotic capabilities of the two, where cribriform DCIS represents a more aggressive form. It seems clear that if the assumptions of this model are correct, then E-Cadherin expression plays a very important role in the morphological patterns discussed previously. This model, however, does have certain drawbacks. Although this model is able to reproduce the comedo-type pattern accurately when the NCN probabilities are shared between 4, 5, and 6, ductal distension would be required to differentiate between solid and comedo DCIS.

This is a distinction that this model does not account for. There is likely some mechanism not described in the literature that differentiates between solid and comedo and papillary and cribriform. These problems as well as the strengths of this model will be investigated in future works.

Acknowledgements

This research is funded in part by the National Science Foundation Award Number ECS 0524042, the Arkansas Biosciences Institute (ABI), and the National Science Foundation GK-12 Fellowship Program.

References

[1] D. Hanahan and R. Weinberg, "The Hallmarks of cancer," *Cell*, vol. 100, pp. 57-70, 2000.

[2] A. Bankhead III, N.S. S. Magnuson, R.B. Heckendorn, "Cellular automaton simulation examining progenitor hierarchy structure effects on mammary ductal carcinoma in situ," *Journal of Theoretical Biology*, vol. 246, pp. 491-498, 2007.

[3] S.J. Franks, H.M. Byrne, J.R. King, J.C.E. Underwood, and C.E. Lewis, "Modelling the early growth of ductal carcinoma in situ," *Journal of Mathematical Biology*, vol. 47, pp. 424-452, 2003.

[4] S.J. Franks, H.M. Byrne, H. Mudhar, J.C.E. Underwood, and C.E. Lewis, "Modelling the growth of comedo ductal carcinoma in situ," *Mathematical Medicine and Biology*, vol. 20, pp. 277-308, 2003.

[5] S.J. Franks, H.M. Byrne, J.C.E. Underwood, and C.E. Lewis, "Biological inferences from a mathematical model of comedo ductal carcinoma in situ of the breast," *Journal of Theoretical Biology*, vol. 232, pp. 523-543, 2005.

[6] Y. Xu, "A free boundary problem model of ductal carcinoma in situ," *Discrete and Continuous Dynamic Systems – Series B*, vol. 4, pp. 337-348, 2004.

[7] B.St. Croix, C. Sheehan, J.W. Rak, V.A. Florenes, J.M. Slingerland, and R.S. Kerbel, "E-Cadherin-dependent growth suppression is mediated by the cyclin-dependent kinase inhibitor p27KIP1," *The Journal of Cell Biology*, vol. 142, no. 2, pp. 557-571, 1998.

[8] S.K. Gupta, A.G. Douglas-Jones, B. Jasani, J.M. Morgan, M. Pignatelli, and R.E. Mansel, "E-Cadherin (E-cad) expression in duct carcinoma in situ (DCIS) of the breast," *Virchows Archive*, vol. 430, pp. 23-28, 1997.

[9] A.G. Naccarato, P. Viacava, G. Bocci, G. Fanelli, P. Aretini, A. Lonobile, G. Montruccoli, and G. Bevilacqua, "Definition of the micro-vascular pattern of the normal human adult mammary gland," *Journal of Anatomy,* vol. 203, pp. 599-603, 2003.

[10] B.C. Sansone, P.P. Delsanto, M. Magnano, M. Scalerandi, "Effects of anatomical constraints on tumor growth," *Physical Review E.*, vol. 64, no. 2, pp. 21903-1-8, 2001.